Published in final edited form as:
Neuroscience. 2008 September 22; 156(1): 129–142. doi:10.1016/j.neuroscience.2008.06.063.

Cholinergic neurons of mouse intrinsic cardiac ganglia contain noradrenergic enzymes, norepinephrine transporters, and the neurotrophin receptors TrkA and p75

Jennifer L. Hoard[1], **Donald B. Hoover**[1], **Abigail M. Mabe**[1], **Randy D. Blakely**[2], **Ning Feng**[3], and **Nazareno Paolocci**[3,4]

1*Department of Pharmacology, James H. Quillen College of Medicine, East Tennessee State University, Johnson City, TN 37614*

2*Center for Molecular Neuroscience and Department of Pharmacology, Vanderbilt University, Nashville, TN, 37232*

3*Division of Cardiology, Johns Hopkins Medical Institutions, Baltimore, MD 21205*

4*Department of Clinical Medicine, Section of General Pathology, University of Perugia, Perugia, Italy*

Abstract

Half of the cholinergic neurons of human and primate intrinsic cardiac ganglia (ICG) have a dual cholinergic/noradrenergic phenotype. Likewise, a large subpopulation of cholinergic neurons of the mouse heart express enzymes needed for synthesis of norepinephrine (NE), but they lack the vesicular monoamine transporter type 2 (VMAT2) required for catecholamine storage. In the present study, we determined the full scope of noradrenergic properties (i.e., synthetic enzymes and transporters) expressed by cholinergic neurons of mouse ICG, estimated the relative abundance of neurons expressing different elements of the noradrenergic phenotype, and evaluated the colocalization of cholinergic and noradrenergic markers in atrial nerve fibers. Stellate ganglia were used as a positive control for noradrenergic markers. Using fluorescence immunohistochemistry and confocal microscopy, we found that about 30% of cholinergic cell bodies contained tyrosine hydroxylase (TH), including the activated form that is phosphorylated at Ser-40 (pSer40 TH). Dopamine β-hydroxylase (DBH) and NE transporter (NET) were present in all cholinergic somata, indicating a wider capability for dopamine metabolism and catecholamine uptake. Yet, cholinergic somata lacked VMAT2, precluding the potential for NE storage and vesicular release. In contrast to cholinergic somata, cardiac nerve fibers rarely showed colocalization of cholinergic and noradrenergic markers. Instead, these labels were closely apposed but clearly distinct from each other. Since cholinergic somata expressed several noradrenergic proteins, we questioned whether these neurons might also contain trophic factor receptors typical of noradrenergic neurons. Indeed, we found that all cholinergic cell bodies of mouse ICG, like noradrenergic cell bodies of the stellate ganglia, contained both tropomyosin-related kinase A (TrkA) and p75 neurotrophin receptors. Collectively, these findings demonstrate that mouse intrinsic cardiac neurons (ICNs), like those of humans, have a complex neurochemical phenotype that goes beyond the classical view of cardiac parasympathetic neurons.

Address correspondence to: Dr. Donald B. Hoover, Department of Pharmacology, College of Medicine, East Tennessee State University, Johnson City, TN 37614, Phone: (423) 439-6322, Fax: (423) 439-8773, E-mail: hoover@etsu.edu.
Dr. Charles R. Gerfen, Neuroanatomy Section Editor

They also suggest that neurotrophins and local NE synthesis might have important effects on neurons of the mouse ICG.

Keywords

cardiac ganglia; choline transporter; vesicular acetylcholine transporter; parasympathetic; sympathetic; heart

INTRODUCTION

The ICG contain postganglionic parasympathetic neurons that provide cholinergic innervation to the heart. These ganglia are located primarily within the atrial epicardium (Ardell, 1994; Ardell, 2004; Parsons, 2004; Al et al., 2007), and their principal neurons contain choline acetyltransferase (ChAT) (Parsons, 2004; Mabe et al., 2006), which is required for the synthesis of acetylcholine (ACh). In contrast, postganglionic cardiac sympathetic neurons occur along with non-cardiac sympathetic neurons in the middle cervical, mediastinal, and stellate ganglia within the chest cavity (Ardell, 1994; Richardson et al., 2006). Most of these sympathetic neurons contain TH (Maslyukov et al., 2006), which is required for the synthesis of NE. While the ICG were initially regarded as simple relay stations in the vagal efferent pathway to the heart, several reports have shown that they form a complex network which integrates input from multiple sources including vagal efferent neurons, extrinsic sympathetic neurons, vagal afferent neurons, and spinal afferent neurons (Ardell, 1994; Pauza et al., 1997; Smith 1999; Pauza et al., 2000; Adams and Cuevas, 2004; Ardell, 2004; Parsons, 2004). Moreover, substantial heterogeneity occurs within the ICN population. In addition to staining for the cholinergic marker ChAT, subpopulations of ICNs differ in: 1) morphology and electrical properties (Edwards et al., 1995), 2) presence of neuropeptides and other non-cholinergic markers (Steele et al., 1994; Horackova et al., 1999; Richardson et al., 2003; Parsons, 2004; Weihe et al., 2005), and 3) targets within the heart (Ardell, 1994; Ardell, 2004; Harrison et al., 2005). Recent work has demonstrated interganglionic connections in the cat heart and shown that these local circuit neurons affect heart rate indirectly (Gray et al., 2004). Further evidence suggests that the neurochemical complexity of ICNs influences function. For example, nitric oxide serves as a co-transmitter that modulates release of ACh from cardiac nerves (Conlon et al., 1996; Herring and Paterson, 2001), while vasoactive intestinal polypeptide has cardiac actions that counteract effects of ACh (Henning and Sawmiller, 2001).

The noradrenergic marker TH has been localized to ICNs of adult rats and guinea-pigs in some studies (Horackova et al., 1999; Horackova et al., 2000; Moravec et al., 1990), but not in others (Forsgren et al.,1990; Leger et al., 1999; Richardson et al., 2003; Steele et al., 1994). Several of the latter investigators did, however, note intense TH immunoreactivity of presumed small intensely fluorescent cells (SIF cells) and sympathetic nerve fibers in the same preparations. In contrast, there is solid and uniform evidence that many human ICNs express all of the enzymes required for synthesis of NE (Singh et al., 1999; Weihe et al., 2005). Furthermore, VMAT2 was also present in a sizable subpopulation of ICNs in humans and nonhuman primates, suggesting that these neurons can store and release NE (Weihe et al., 2005). Whether ICNs also express NET is unknown. The fact that many ICNs of humans and other primates have a dual cholinergic/noradrenergic phenotype (Weihe et al., 2005) is intriguing in view of evidence that neonatal sympathetic neurons exhibit such a dual phenotype when maintained in co-culture with cardiac myocytes (Furshpan et al., 1976). Under this condition, they are capable of rapidly switching from release of NE to ACh in response to trophic factor stimulation of the p75 neurotrophin receptor (Yang et al., 2002).

Understanding the nature of cardiac innervation in the mouse is important not only because this species is used widely in cardiovascular research, but also because it closely resembles the human neurochemical phenotype. We have reported that all ICNs of adult mice exhibit the cholinergic phenotype, i.e. staining for ChAT (Mabe et al., 2006). Furthermore, these neurons expressed receptors for neurturin (Mabe et al., 2006), which is a trophic factor required for normal development of cardiac cholinergic innervation (Hiltunen et al., 2000). Others have reported that many ICNs of the mouse, like those of humans and nonhuman primates, also expressed TH and other enzymes that are required for synthesis of NE (Weihe et al., 2005). However, mouse ICNs lacked VMAT2, suggesting that they could not store or release NE (Weihe et al., 2005).

This study was conducted to further define the neurochemical phenotypes of mouse ICNs and nerve fibers and to compare these characteristics with those displayed by sympathetic neurons of the stellate ganglia. Our findings confirmed the presence of TH in a subpopulation of mouse ICNs and showed that some TH occurs as the activated form. Moreover, we obtained novel evidence that most ICNs express NET. Finally, we observed that all mouse ICNs contained TrkA and p75 neurotrophin receptors, which are typically associated with sympathetic neurons. Possible functional implications of these findings were discussed.

EXPERIMENTAL PROCEDURES

Animals

A total of 18 mice were used for this study. Fifteen adult male C57BL/6 mice (24–30g) were obtained from Harlan Sprague Dawley, Inc. (Indianapolis, IN). Two *p75 (−/−)* mice and one *p75 (+/+)* littermate were obtained by breeding of *p75 (+/−)* mice purchase from The Jackson Laboratory (Bar Harbor, ME; http://jaxmice.jax.org/strain/002213_3.html). Animal protocols were approved by the East Tennessee State University Committee on Animal Care or the Johns Hopkins Animal Care Committee and conformed to guidelines of the National Institutes of Health as published in the *Guide for the Care and Use of Laboratory Animals* (NIH publication No. 85-23, revised 1996).

Tissue collection and preparation

Animals were deeply anesthetized with 5% isoflurane and euthanized by cervical dislocation. Hearts were removed rapidly and perfused through the ascending aorta with 3 ml of phosphate buffered saline (PBS) (pH 7.4, room temperature) followed by 3 ml of cold fixative comprising 4% paraformaldehyde and 0.2% picric acid in PBS. Tissues were post-fixed for another 2h at 4°C, cryoprotected for 2 days in cold 20% sucrose/PBS, and sectioned in a Leica cryostat/microtome. Stellate ganglia were removed from four mice, immersed in cold fixative for 4h, and processed in the same manner as hearts. Serial 16μm short-axis sections of hearts were collected in six sets beginning at the most superior aspect of the atria and ending at a level well into the ventricular myocardium. Adjacent sections in each set were separated by an 80 μm space corresponding to five sections used for other sets. Stellate ganglia were sectioned at the same thickness. Each set of slides was boxed separately, wrapped in aluminum foil, and stored at −20°C.

Immunohistochemistry

Slide-mounted tissue sections were immunostained at room temperature. Sections were washed 4 times in 0.1M PBS (pH 7.3) (10 min each), permeabilized with 0.4% Triton X-100 in PBS containing 0.5% bovine serum albumin (BSA) (20 min), and blocked for 2h in PBS containing 10% normal donkey serum (Jackson ImmunoResearch Laboratories, West Grove, PA), 1% BSA, and 0.4% Triton X-100. Tissues were then incubated for 15–18h with two primary antisera generated in different species (Table 1), washed four times with 0.1M PBS (10 min

each), permeabilized with 0.4% Triton X-100 in PBS containing 0.5% BSA, and incubated for 2h with two species specific secondary antibodies (Table 1). After washing the sections four times with PBS (10 min each), coverglasses were attached using Citifluor mounting medium (Ted Pella, Inc., Redding, CA) and sealed with clear nail polish. Representative sections were routinely processed without primary antibodies (negative control). In all cases, these negative control sections showed only background fluorescence. Each combination of markers was evaluated using sets of sections from at least three C57BL/6 mice. The specificity of staining for p75 was evaluated using sections from two *p75 (−/−)* mice and one *p75 (+/+)* littermate.

Confocal microscopy and image analysis

Labeled tissue sections were viewed initially using an Olympus BX41 microscope, and regions of interest were selected for further evaluation using a Leica TCS SP2 confocal microscope system. Specimens were scanned sequentially to avoid crosstalk between fluorochromes, and a maximum projection image was obtained from each series of optical sections. Colocalization of immunolabels was evaluated in overlay images obtained from these scans. Negative controls for each fluorochrome were also scanned using the same parameter settings. Images were exported into Corel Draw 11 and adjusted for brightness and contrast. The number of ICNs labeled for either protein gene product 9.5 (PGP 9.5) alone or for PGP 9.5 and TH were counted in digital images collected with an Optronics MagnaFire SP CCD camera mounted on the Olympus BX41 microscope. Cell counts were performed using Stereo Investigator/ Workstation software (MicroBrightField, Williston, VT), and values are presented as the mean ± SE for percentage of neurons that were TH-positive.

RESULTS

Mouse ICNs exhibit cholinergic phenotype

The ICG of mice are located in the atrial epicardium, especially near the midline along the posterior surface (Fig. 1A) but also at other sites as recently reported by Al et al. (2007). The parasympathetic neurons of the ICG showed distinct staining for the pan-neuronal marker PGP 9.5 (Fig. 1A and B) and prominent ChAT immunoreactivity throughout their cytosol (Fig. 1C). Robust staining for ChAT also revealed numerous ChAT-immunoreactive (ChAT-IR) smooth and varicose nerve processes within the ganglia; these processes frequently came into close apposition with the ChAT-IR perikarya (Fig. 1C and insert). This pattern supports the classical view of postganglionic cholinergic neurons innervated by vagal preganglionic cholinergic nerves. Further evidence of the cholinergic phenotype came from double labeling of sections for high affinity choline transporter (CHT) and vesicular ACh transporter (VAChT). Sequential confocal scanning of these preparations demonstrated that CHT and VAChT were highly colocalized in varicose nerves that surround many ICNs and to nerve fibers within the atrial myocardium (Fig. 1D–F). The precise colocalization of CHT and VAChT is evident from the predominance of yellow in the overlay image (Fig. 1F).

A subpopulation of ICNs contains the noradrenergic marker TH

A sizable subpopulation of mouse ICNs also displayed TH immunoreactivity (Fig. 2A and B), confirming a previous report by Weihe et al. (2005). This finding was duplicated using two TH antibodies generated in different species. Quantitative evaluation of all ganglia present in three sets of sections double labeled for PGP 9.5 and TH showed that 30 ± 2.1% of mouse ICNs were TH-positive (n=3; total of 1415 PGP 9.5-positive neurons). Furthermore, TH-positive neurons also stained with antibody to the Ser-40 phosphorylated form of TH (pSer40 TH; Fig. 2C and D), suggesting that some of the enzyme had been activated (Fujisawa and Okuno, 2005). Double labeling for CHT and TH showed that some TH-positive neurons received cholinergic innervation (Fig. 2E and F). TH also occurred in SIF cells, which were smaller than ICNs (Fig. 2B)

ICNs contain DBH and NET but lack VMAT2

Using double labeling with antibodies directed against TH and other noradrenergic markers, we sought to determine if additional indicators of the noradrenergic phenotype occurred in ICNs. These experiments showed that all ICNs contained immunoreactivity for DBH (Fig. 3A–C) and NET (Fig. 3D–F). Thus, these markers occurred in neurons that lacked TH immunoreactivity as well as neurons that were TH-positive. The intensity of DBH and NET staining was occasionally greater in the TH-IR somata. Although a few TH-positive neurons exhibited weak VMAT2 staining, the vast majority of ICNs lacked VMAT2 immunoreactivity (Fig. 3G–I). Staining for DBH, NET, and VMAT2 was evident in nerve fibers associated with the ganglia and adjacent tissue. All of these markers were colocalized with TH at these sites (Fig. 3).

Noradrenergic neurons of the stellate ganglia contain TH, NET, and VMAT2

The stellate ganglia contain noradrenergic neurons that are a major source of cardiac sympathetic innervation in rodents (Choate and Feldman, 2003; Richardson et al., 2006). Sections from these ganglia were evaluated so that the staining pattern of known noradrenergic neurons could be compared with that of ICNs. In contrast to ICNs, a vast majority of stellate neurons were immunoreactive for VMAT2 as well as TH and NET (Fig. 4A, B, and D). Punctate staining for VAChT surrounded noradrenergic neurons of the stellate ganglia (Fig. 4C and D), consistent with the known preganglionic cholinergic innervation of these sympathetic neurons.

Colocalization of CHT with VAChT and of TH with VMAT2 in atrial nerve fibers

Cholinergic nerve fibers require CHT to accumulate choline needed for the synthesis of ACh, and VAChT is needed for the vesicular storage of ACh (Ferguson et al., 2003). Double labeling for these cholinergic markers demonstrated that they were colocalized to the same nerve fibers throughout the mouse atria (Fig. 5A–C). Similarly, noradrenergic nerve fibers require TH for the first step in NE synthesis and VMAT2 for NE transport into storage vesicles. Double labeling for these noradrenergic markers demonstrated that they were colocalized to the same nerve fibers in mouse atrium (Fig. 5D–F). The colocalization of cholinergic and noradrenergic markers in their respective nerve fibers is evident from the yellow staining of nerves in the overlay images (Fig. 5C and F).

Cholinergic markers are not colocalized with noradrenergic markers in cardiac nerve fibers

Double labeling for VAChT and either TH or VMAT2 showed that the distribution of VAChT-IR cardiac nerves often paralleled that of TH- and VMAT2-IR nerves (Fig. 6A, B, D, and E). However, careful examination of overlay images from sequential confocal scans showed that the cholinergic and noradrenergic markers were closely apposed (Fig. 6C and F) but very rarely colocalized as seen when double labeling was performed with matched cholinergic or noradrenergic markers (Fig. 5). Likewise, cholinergic and noradrenergic markers were not colocalized in nerves fibers within the ICG (Fig. 6D–F).

Stellate ganglion neurons and ICNs are immunoreactive for neurotrophin receptors

Since ICNs had several elements of the noradrenergic phenotype, we hypothesized that they would also contain neurotrophic factor receptors that have been associated with noradrenergic sympathetic neurons (Klein, 1994; Roux and Barker, 2002). Accordingly, we performed parallel immunohistochemical experiments to evaluate TrkA and p75 receptor immunoreactivity of sections from stellate ganglia and ICG. Double labeling for TH and TrkA showed that all TH-IR neurons of the stellate ganglion also showed TrkA immunoreactivity (Fig. 7A and B). Identical experiments with ICG revealed that TH-positive and TH-negative ICNs were TrkA-IR (Fig. 7C and D). In contrast, cardiac nerve fibers were not TrkA-IR.

Analogous double labeling experiments with antibodies for TH and p75 receptor showed p75 immunoreactivity associated with all neurons in both ganglia (Fig. 8). Labeling for this receptor was particularly intense at the perimeter of ICNs (Fig. 8D) but also occurred in the cytosol (Fig. 9B). The p75 antibody also labeled cardiac nerve fibers. Specific staining for p75 receptor was absent in sections of heart from a *p75 receptor* (−/−) mouse but TH-IR ICNs and nerve fibers were still present (Fig. 9).

DISCUSSION

Our study provides novel and confirmatory evidence concerning the neurochemical phenotype of ICNs and their postganglionic elements in the mouse heart (Fig. 10). Here we confirmed that a sizable subpopulation of mouse ICNs contains TH (Weihe et al., 2005) while showing for the first time that some TH in these neurons occurs in the activated form (i.e., pSer40 TH). Also new was the observation that all ICNs stain for two additional noradrenergic makers, DBH and NET, with a NET staining intensity comparable to that observed in noradrenergic neurons of the stellate ganglia. Our results confirmed that ICNs lack VMAT2 (Weihe et al., 2005), which is an essential requirement for storage and synaptic release of NE. As for postganglionic nerve fibers in the atrium, we found no colocalization of TH with VAChT, but each of these markers was colocalized with matched noradrenergic or cholinergic markers as expected for cholinergic and noradrenergic nerves (Fig. 10). Lastly, we made the new observation that TrkA and p75 neurotrophin receptors are present in all mouse ICNs.

Mouse ICNs and many atrial nerve fibers show the expected cholinergic phenotype

This study demonstrated that all ICNs and many atrial nerve fibers in the mouse heart showed evidence of the cholinergic neurochemical phenotype, which was expected for cardiac parasympathetic neurons. Specifically, all neural somata were ChAT-IR, and CHT was colocalized with VAChT in terminal processes within the myocardium. This colocalization was established by sequential confocal scanning, which showed extensive overlap of these markers. Labeling of cardiac cholinergic nerve fibers with the ChAT antibody proved variable in the present and previous studies (Hoover et al., 2004; Mabe et al., 2006), although we were able to demonstrate colocalization of CHT with ChAT in nerve fibers at the sinoatrial node of guinea pig (Hoover et al., 2004). More recent evidence suggests that the limited sensitivity of this ChAT antibody can be attributed to its preference for the conventional isoform of ChAT over the peripheral isoform, which is most abundant in the heart (Yasuhara et al., 2007). In accord with our previous studies of guinea-pig heart (Hoover et al., 2004), we found that CHT immunoreactivity was absent or weak in cholinergic somata of the mouse ICG. Weak staining of cholinergic cell bodies for CHT and VAChT could be attributed to transport of these proteins to cholinergic nerve fibers in the myocardium, where staining was intense. This argument is supported by evidence that colchicine treatment increases CHT immunoreactivity of guinea-pig ICNs maintained in culture (Hoover et al, 2004). Cholinergic markers including ChAT also occurred in varicose processes that surrounded most ICNs. This staining was probably associated with preganglionic vagal innervation since cholinergic input from other extrinsic sources (i.e., preganglionic sympathetic neurons) has not been reported. Previous work with guinea-pig ICG showed that cholinergic innervation was lost after several days in culture, suggesting that cholinergic input had an extrinsic source rather than originating from neurons in the same or different ICG (Hoover et al., 2004; Parsons 2004). In contrast, recent work has demonstrated the presence and function of interganglionic projections in the cat heart (Gray et al., 2004). We cannot rule out the possibility that ICG are linked by local circuit neurons in the mouse.

Cholinergic somata of the ICG contain several noradrenergic markers but lack VMAT2

A previous investigation showed that a subpopulation of neurons in mouse ICG contained TH but lacked VMAT2 (Weihe et al., 2005). The presence of other enzymes required for NE synthesis (i.e., aromatic amino acid decarboxylase and DBH) was also noted but the abundance of ICNs that contained these markers was not specified. We used three separate antibodies to confirm the presence of TH in a subpopulation of mouse ICNs. This was an important issue since previous studies have reported that TH-positive neurons do not occur in adult rat or guinea-pig ICG (Steele et al., 1994; Leger et al., 1999; Richardson et al., 2003). Instead, these investigators observed TH staining of SIF cells, whose function remains unknown (Leger et al., 1999). In pilot experiments, we performed double labeling with TH antibodies that were generated in different species (not shown) and found that both antibodies labeled identical ICNs, cardiac nerves, and SIF cells in the mouse. In the present study, we found that TH was restricted to a subpopulation of mouse ICNs but all ICNs showed DBH and NET immunoreactivity. Nevertheless, we found that mouse ICNs lacked VMAT2, as reported previously in work that used a different primary antibody to VMAT2 (Weihe et al., 2005). The effectiveness of our antibody was demonstrated by positive VMAT2 staining of TH-IR sympathetic neurons in the stellate ganglion and TH-IR nerve fibers in the atrium. Collectively, our data and earlier work by Weihe et al. (2005) provide clear-cut evidence that a sizable subpopulation of mouse ICNs contain all of the enzymes required for the synthesis of NE and that all ICNs contain NET and DBH but lack VMAT2.

Noradrenergic marker are not localized to cholinergic nerve fibers in the atria

While TH was clearly abundant in the cell bodies of many ICNs, neither TH nor VMAT2 was detected in cholinergic nerve processes within the myocardium. Support for this conclusion came from double labeling experiments that used different combinations of antibodies to cholinergic and noradrenergic markers. Sequential scanning of these sections showed colocalization of CHT with VAChT in presumed cholinergic nerve fibers and colocalization of TH with VMAT2 in noradrenergic fibers, but VAChT was rarely colocalized with TH or VMAT2. Instead, these markers were juxtaposed very closely but not colocalized. The presence of TH immunoreactivity in the soma but not in terminal varicosities of cardiac cholinergic neurons suggests that TH is made but not exported. Lack of TH export might explain the observation that many TH-positive neurons of the ICG stained more intensely than noradrenergic neurons of the stellate ganglia. Recent work in *C. elegans* has shown that VMAT2 and the dopamine transporter (DAT) use different pathways for trafficking to nerve terminals and that a carboxy-terminal sequence targets DAT for export (McDonald et al., 2007). Accordingly, ICNs and stellate ganglion neurons may differ in the presence of one or more factors that direct the export or retention of TH. The present findings with normal tissue do not exclude the possibility that noradrenergic markers could occur in cardiac cholinergic nerve fibers under pathophysiological conditions. We have reported that about 21% of dissociated mouse ICNs express TH immunoreactivity when maintained in culture (Hoard et al., 2007). These neurons were axotomized during the dissociation process, and under this condition, both the somata and neurites were TH-IR.

The absence of VMAT2 in ICNs and atrial cholinergic nerve fibers suggests that these neurons lack the ability for vesicular storage and release of catecholamines. This view is consistent with data obtained in isolated mouse atria showing that vagal stimulation caused bradycardia that was blocked by atropine (Choate and Feldman, 2003). Vagal stimulation during muscarinic blockade with atropine did not cause tachycardia. Likewise, vagal stimulation caused bradycardia in our preliminary experiments with anesthetized mice but had no effect on heart rate after treatment with atropine.

Anatomical evidence for crosstalk between noradrenergic and cholinergic systems

The close proximity of cholinergic and noradrenergic nerve fibers that we observed in mouse atrial muscle would be expected to foster prejunctional crosstalk, which has been demonstrated in other species and shown to influence neural regulation of cardiac function (Levy and Warner, 1994). Our studies also showed close apposition of cholinergic and noradrenergic varicosities within the mouse ICG, and this finding suggests another opportunity for crosstalk between these systems. Others have demonstrated noradrenergic innervation of guineapig and rat ICG (Leger et al., 1999; Richardson et al., 2003; Parsons, 2004), and in guinea pigs TH was colocalized with neuropeptide Y (NPY). The TH-/NPY-IR nerves in guinea-pig ICG had an extrinsic source as they were absent in ganglia maintained several days in culture (Parsons 2004). The VMAT2-IR noradrenergic nerve fibers in mouse ICG probably have an extrinsic origin as well since mouse ICNs lack VMAT2. Presynaptic interactions have not been evaluated at the level of ICG but NE and NPY both have postsynaptic effects on a subpopulation of ICNs in the guinea pig (Parsons, 2004). The SIF cells that we identified in mouse ICG are another source for NE. These cells were smaller than TH-positive ICNs and did not stain strongly for PGP 9.5 (unpublished observation). We found no evidence for a direct contact between SIF cells and ICNs. Likewise, confocal analysis of SIF cells in guinea-pig ICG showed that they had only short processes that lacked varicosities (Leger et al., 1999).

Possible functions of noradrenergic enzymes and NET in cholinergic somata

It is unclear why cholinergic neurons of the mouse heart also express some noradrenergic markers, but there are several possible explanations. First, these proteins could be a holdover from development. Evaluation of postnatal development of the rat intrinsic cardiac nervous system has shown that a majority of neurons stained strongly for TH at ≤ two weeks of age (Horackova et al., 2000). This TH immunoreactivity decreased over the next three weeks as ChAT immunoreactivity became dominant. Perhaps neonatal mouse ICNs exhibit a similar TH phase that persists in some mature neurons. Second, the presence of NET could enable uptake of catecholamines by ICNs. Catecholamines might enter the interstitial fluid of the ICG after release from the adrenal medulla, noradrenergic nerve fibers present within the ICN (see Fig. 2, Fig. 3, Fig. 6D, and Fig. 8C), and SIF cells. Since ICNs lack VMAT2, accumulated catecholamines would be subject to degradation by monoamine oxidase, which occurs in most guinea-pig ICNs (Baluk and Gabella, 1990). Lastly, TH-positive neurons of the ICG might have an autocrine or paracrine function. In this scenario, catecholamines would exit the neurons by reverse transport using NET and stimulate neuronal adrenergic receptors, which have been identified by intracellular microelectrode recordings from ICNs (Smith, 1999; Adams and Cuevas, 2004; Parsons, 2004). Carrier-mediated release of NE from sympathetic nerves is known to occur during myocardial ischemia and contributes significantly to excessive noradrenergic stimulation and associated cardiac dysfunction (Schömig et al., 1987; Schömig et al., 1991). Under this condition, intraneuronal acidosis activates the Na^+/H^+ exchanger, which increases $[Na^+]_i$ and in turn triggers reversal of NET (Hatta et al., 1997; Smith and Levi, 1999). Analogous processes might trigger release of NE from the somata of ICNs during ischemia.

Potential significance of neurotrophin receptors in mouse ICNs

This study provides the first evidence that ICNs of adult mice contain TrkA and p75 neurotrophin receptors. TrkA is the high affinity receptor for nerve growth factor (NGF), and has a well-established role in sympathetic neurons and a large subpopulation of sensory neurons (Klein, 1994; Roux and Barker, 2002). NGF is a target-derived survival factor for these neurons and has additional effects to stimulate neurite outgrowth, maintain adult neurons and their processes, and to modulate synaptic properties. Activation of TrkA at nerve endings by NGF has local effects, but the TrkA-NGF complex is also internalized and transported back to the

neuronal cell body where it affects gene transcription and promotes survival. Deletion of the TrkA gene causes major deficits in the number of sympathetic and sensory neurons but it is believed that parasympathetic neurons are unaffected (Klein, 1994). Recent work showed that members of the glial cell line-derived neurotrophic factor family of ligands have a dominant role as trophic factors for development of parasympathetic neurons (Airaksinen and Saarma, 2002). More specifically, neurturin was established as the target-derived trophic factor required for normal cholinergic innervation of the heart (Hiltunen et al., 2000). Nevertheless, neurturin cannot be the sole trophic factor for ICNs since hearts from neurturin knockout mice still had about 20% the normal number of cholinergic neurons (Mabe and Hoover, 2008). The presence of TrkA in mouse ICNs suggests that NGF might have a role in survival of at least a subpopulation of these parasympathetic neurons.

The p75 receptor also occurs in sympathetic and sensory neurons where it complexes with TrkA to increase the specificity and affinity of TrkA for NGF (Klein, 1994; Roux and Barker, 2002). However, under certain conditions p75 can inhibit neurite outgrowth and induce apoptosis (Roux and Barker, 2002). While p75 is not required for survival of sympathetic neurons (Klein, 1994), recent evidence demonstrated that p75 knockout mice have a reduced density of noradrenergic nerves in the atria and impaired noradrenergic regulation of heart rate (Habecker et al., 2008). Cholinergic nerve density and the heart rate response to atropine were unaffected in p75 knockout mice, suggesting that ICNs do not have a similar requirement for p75.

The presence of TrkA and p75 in adult ICNs suggests that these neurons could be affected by NGF. Little is known about the response of adult parasympathetic neurons to trophic factors but recent work demonstrated that NGF (100 ng/ml) can stimulate dendritic growth in airway cholinergic neurons of adult guinea pigs (Hazari et al., 2007). Furthermore, NGF (10 and 100 ng/ml) caused a rapid-onset potentiation of synaptic efficacy and nicotinic responses of airway parasympathetic neurons (Hazari et al., 2007). Such changes in NGF levels are most likely to occur under pathophysiological conditions. Regional elevation of NGF after myocardial infarction is associated with heterogeneous sprouting of noradrenergic nerves, which is thought to increase risk for fatal arrhythmias (Zhou et al., 2004). Conversely, reduced levels of myocardial NGF can occur in heart failure (Kaye et al., 2000) and diabetes (Hellweg and Hartung, 1990), resulting in loss of noradrenergic nerves that support inotropic function. The presence of TrkA and p75 receptors on ICNs suggests that these neurons might have the potential for remodeling if neurotrophin availability is altered.

Abbreviations

ACh, acetylcholine
BSA, bovine serum albumin
CHT, high affinity choline transporter
ChAT, choline acetyltransferase
DBH, dopamine β-hydroxylase
DAT, dopamine transporter
ICG, intrinsic cardiac ganglia
ICN, intrinsic cardiac neuron
IR, immunoreactive
KO, knockout
NGF, nerve growth factor
NE, norepinephrine
NET, norepinephrine transporter
NPY, neuropeptide Y
PBS, phosphate buffered saline

PGP 9.5, protein gene product 9.5
SIF cells, small intensely fluorescent cells
TrkA, tropomyosin-related kinase A
VAChT, vesicular ACh transporter
VMAT2, vesicular monoamine transporter type 2
WT, wild-type

Acknowledgments

This work was supported by a Grant-in-Aid from the AHA Southeast Affiliate (DBH), NIH HL056693 and MH073159 (RDB), a Scientist-Development-Grant from AHA Mid-Atlantic Affiliate and NIH HL075265 (NP). Abigail Mabe was supported by a Predoctoral Fellowship from the AHA Southeast Affiliate.

REFERENCES

Adams, DJ.; Cuevas, J. Electrophysiological properties of intrinisc cardiac neurons. In: Armour, JA.; Ardell, JL., editors. Basic and Clinical Neurocardiology. New York: Oxford University Press; 2004. p. 1-60.

Airaksinen MS, Saarma M. The GDNF family: signaling, biological functions and therapeutic value. Nat Rev Neurosci 2002;5:383–394. [PubMed: 11988777]

Al J, Epstein PN, Gozal D, Yang B, Wurster R, Cheng ZJ. Morphology and topography of nucleus ambiguus projections to cardiac ganglia in rats and mice. Neuroscience 2007;149:845–860. [PubMed: 17942236]

Ardell, JL. Structure and function of mammalian intrinsic cardiac neurons. In: Armour, JA.; Ardell, JL., editors. Neurocardiology. New York: Oxford University Press; 1994. p. 95-114.

Ardell, JL. Intrathoracic neuronal regulation of cardiac function. In: Armour, JA.; Ardell, JL., editors. Basic and Clinical Neurocardiology. New York: Oxford University Press; 2004. p. 118-152.

Baluk P, Gabella G. Some parasympathetic neurons in the guinea-pig heart express aspects of the catecholaminergic phenotype in vivo. Cell Tissue Res 1990;261:275–285. [PubMed: 1976043]

Choate JK, Feldman R. neuronal control of heart rate in isolated mouse atria. Am J Physiol heart Circ Physiol 2003;285:H1340–H1346. [PubMed: 12738615]

Conlon K, Collins T, Kidd C. Modulation of vagal actions on heart rate produced by inhibition of nitric oxide synthase in the anaesthetized ferret. Exp Physiol 1996;81:547–550. [PubMed: 8737087]

Edwards FR, Hirst GD, Klemm MF, Steele PA. Different types of ganglion cell in the cardiac plexus of guinea-pigs. J Physiol (Lond) 1995;486:453–471. [PubMed: 7473210]

Ferguson SM, Savchenko V, Apparsundaram S, Zwick M, Wright J, Heilman CJ, Yi H, Levey AI, Blakely RD. Vesicular localization and activity-dependent trafficking of presynaptic choline transporters. J Neurosci 2003;23:9697–9703. [PubMed: 14585997]

Forsgren S, Moravec M, Moravec J. Catecholamine-synthesizing enzymes and neuropeptides in rat heart epicardial ganglia; an immunohistochemical study. Histochem J 1990;22:667–676. [PubMed: 1706694]

Fujisawa H, Okuno S. Regulatory mechanism of tyrosine hydroxylase activity. Biochem Biophys Res Commun 2005;338:271–276. [PubMed: 16105651]

Furshpan EJ, MacLeish PR, O'Lague PH, Potter DD. Chemical transmission between rat sympathetic neurons and cardiac myocytes developing in microcultures: evidence for cholinergic, adrenergic, and dual-function neurons. Proc Natl Acad Sci USA 1976;73:4225–4229. [PubMed: 186792]

Habecker BA, Bilimoria P, Linick C, Gritman K, Lorentz CU, Woodward W, Birren SJ. Regulation of cardiac innervation and function via the p75 neurotrophin receptor. Auto Neurosci Basic Clin. 2008

Harrison TA, Perry KM, Hoover DB. Regional cardiac ganglia projections in the guinea pig heart studied by postmortem DiI tracing. Anat Rec A Discov Mol cell Evol Biol 2005;285:758–770. [PubMed: 15977223]

Hatta E, Yasuda K, Levi R. Activation of histamine H_3 receptors inhibits carrier-mediated norepinephrine release in a human model of protracted myocardial ischemia. J Pharmacol Exp Ther 1997;283:494–500. [PubMed: 9353362]

Hazari MS, Pan JH, Myers AC. Nerve growth factor acutely potentiates synaptic transmission in vitro and induces dendritic growth in vivo on adult neurons in airway parasympathetic ganglia. Am J Physiol Lung Cell Mol Physiol 2007;292:L992–L1001. [PubMed: 17158596]

Hellweg R, Hartung HD. Endogenous levels of nerve growth factor (NGF) are altered in experimental diabetes mellitus: a possible role for NGF in the pathogenesis of diabetic neuropathy. J Neurosci Res 1990;26:258–267. [PubMed: 2142224]

Henning RJ, Sawmiller DR. Vasoactive intestinal peptide: cardiovascular effects. Cardiovasc Res 2001;49:27–37. [PubMed: 11121793]

Herring N, Paterson DJ. Nitric oxide-cGMP pathway facilitates acetylcholine release and bradycardia during vagal nerve stimulation in the guinea-pig in vitro. J Physiol 2001;535:507–518. [PubMed: 11533140]

Hiltunen JO, Laurikainen A, Airaksinen MS, Saarma M. GDNF family receptors in the embryonic and postnatal rat heart and reduced cholinergic innervation in mice hearts lacking ret or GFRa2. Dev Dyn 2000;219:28–39. [PubMed: 10974669]

Hoard JL, Hoover DB, Wondergem R. Phenotypic properties of adult mouse intrinsic cardiac neurons maintained in culture. Am J Physiol Cell Physiol 2007;293:C1875–C1883. [PubMed: 17913847]

Hoover DB, Ganote CE, Ferguson SM, Blakely RD, Parsons RL. Localization of cholinergic innervation in guinea pig heart by immunohistochemistry for high-affinity choline transporters. Cardiovasc Res 2004;62:112–121. [PubMed: 15023558]

Horackova M, Armour JA, Byczko Z. Distribution of intrinsic cardiac neurons in whole-mount guinea pig atria identified by multiple neurochemical coding. A confocal microscope study. Cell Tissue Res 1999;297:409–421. [PubMed: 10460488]

Horackova M, Slavikova J, Byczko Z. Postnatal development of the rat intrinsic cardiac nervous system: a confocal laser scanning microscopy study in whole-mount atria. Tissue Cell 2000;32:377–388. [PubMed: 11201277]

Kaye DM, Vaddadi G, Gruskin SL, Du XJ, Esler MD. Reduced myocardial nerve growth factor expression in human and experimental heart failure. Circ Res 2000;86:E80–E84. [PubMed: 10764418]

Klein R. Role of neurotrophins in mouse neuronal development. FASAB J 1994;8:738–744.

Leger J, Croll RP, Smith FM. Regional distribution and extrinsic innervation of intrinsic cardiac neurons in the guinea pig. J Comp Neurol 1999;407:303–317. [PubMed: 10320213]

Levy, MN.; Warner, MR. Parasympathetic effects on cardiac function. In: Armour, JA.; Ardell, JL., editors. Neurocardiology. New York: Oxford University Press; 1994. p. 53-76.

Maslyukov PM, Shilkin VV, Timmermans JP. Immunocytochemical characteristics of neurons in the stellate ganglion of the sympathetic trunk in mice during postnatal ontogenesis. Neurosci Behav Physiol 2006;36:41-11.

Mabe AM, Hoard JL, Duffourc MM, Hoover DB. Localization of cholinergic innervation and neurturin receptors in adult mouse heart and expression of the neurturin gene. Cell Tissue Res 2006;326:57–67. [PubMed: 16708241]

Mabe AM, Hoover DB. Structural and functional cardiac cholinergic deficits in adult neurturin knockout mice. FASEB J 2008;22:1230.9.

McDonald PW, Hardie SL, Jessen TN, Carvelli L, Matthies DS, Blakely RD. Vigorous motor activity in *Caenorhabditis elegans* requires efficient clearance of dopamine mediated by synaptic localization of the dopamine transporter DAT-1. J Neurosci 2007;27:14216–14227. [PubMed: 18094261]

Moravec M, Moravec J, Forsgren S. Catecholaminergic and peptidergic nerve components of intramural ganglia in the rat heart. An immunohistochemical study. Cell Tissue Res 1990;262:315–327. [PubMed: 1706221]

Parsons, RL. Mammalian cardiac ganglia as local integration centers: histochemical and electrophysiological evidence. In: Dun, NJ.; Machado, BH.; Pilowsky, PM., editors. Neural Mechanisms of Cardiovascular Regulation. Boston: Kluwer Academic Publishers; 2004. p. 335-356.

Pauza DH, Skripka V, Pauziene N, Stropus R. Morphology, distribution, and variability of the epicardiac neural ganglionated subplexuses in the human heart. Anat Rec 2000;259:353–382. [PubMed: 10903529]

Pauza DH, Skripkiene G, Skripka V, Pauziene N, Stropus R. Morphological study of neurons in the nerve plexus on heart base of rats and guinea pigs. J Auton Nerv Syst 1997;62:1–12. [PubMed: 9021644]

Richardson RJ, Grkovic I, Anderson CR. Immunohistochemical analysis of intracardiac ganglia of the rat heart. Cell Tissue Res 2003;314:337–350. [PubMed: 14523644]

Richardson RJ, Grkovic I, Allen AM, Anderson CR. Separate neurochemical classes of sympathetic postganglionic neurons project to the left ventricle of the rat. Cell Tissue Res 2006;324:9–16. [PubMed: 16418838]

Roux PP, Barker PA. Neurotrophin signaling through p75 neurotrophin receptor. Prog Neurobiol 2002;67:203–233. [PubMed: 12169297]

Schömig A, Fischer S, Kurz T, Richardt G, Schömig E. Nonexocytotic release of endogenous noradrenaline in the ischemic and anoxic rat heart: mechanism and metabolic requirements. Circ Res 1987;60:194–205. [PubMed: 3568291]

Schömig A, Haass M, Richardt G. Catecholamine release and arrhythmias in acute myocardial ischaemia. Eur Heart J 1991;12:38–47. [PubMed: 1804638]

Singh S, Johnson PI, Javed A, Gray TS, Lonchyna VA, Wurster RD. Monoamine- and histamine-synthesizing enzymes and neurotransmitters within neurons of adult human cardiac ganglia. Circulation 1999;99:411–419. [PubMed: 9918529]

Smith FM. Extrinsic inputs to intrinsic neurons in the porcine heart in vitro. Am J Physiol Regul Integr Comp Physiol 1999;276:R455–R467.

Smith NCE, Levi R. LLC-PK1 cells stably expressing the human norepinephrine transporter: a functional model of carrier-mediated norepinephrine release in protracted myocardial ischemia. J Pharmacol Exp Ther 1999;291:456–463. [PubMed: 10525059]

Steele PA, Gibbins IL, Morris JL, Mayer B. Multiple populations of neuropeptide-containing intrinsic neurons in the guinea-pig heart. Neuroscience 1994;62:241–250. [PubMed: 7816202]

Weihe E, Schutz B, Hartschuh W, Anlauf M, Schafer MK, Eiden LE. Coexpression of cholinergic and noradrenergic phenotypes in human and nonhuman autonomic nervous system. J Comp Neurol 2005;492:370–379. [PubMed: 16217790]

Yang B, Slonimsky JD, Birren SJ. A rapid switch in sympathetic neurotransmitter release properties mediated by the p75 receptor. Nat Neurosci 2002;5:539-5445. [PubMed: 11992117]

Yasuhara O, Matsuo A, Bellier JP, Aimi Y. Demonstration of choline acetyltransferase of a peripheral type in the rat heart. J Histochem Cytochem 2007;55:287–299. [PubMed: 17142806]

Zhou S, Chen LS, Miyauchi Y, Miyauchi M, Kar S, Kangavari S, Fishbein MC, Sharifi B, Chen PS. Mechanisms of cardiac nerve sprouting after myocardial infarction in dogs. Circ Res 2004;95:76–83. [PubMed: 15166093]

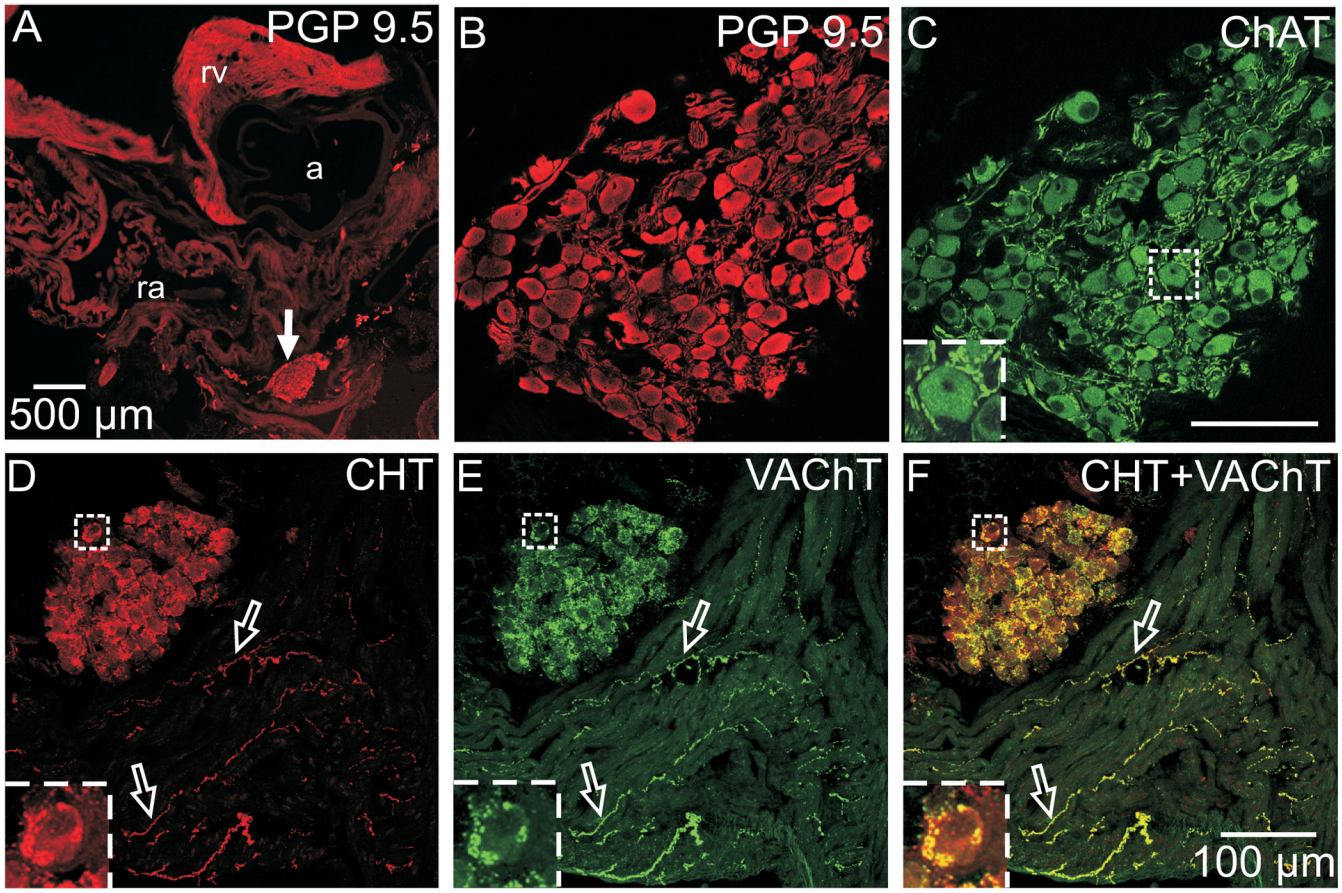

Fig. 1. ICNs exhibit the cholinergic phenotype

(A) Low magnification epifluorescence image of atrial section stained for the pan-neuronal marker PGP 9.5. Arrow indicates the location of a ganglion shown at higher magnification in confocal images (B) and (C). PGP 9.5-IR neuronal cell bodies (A, B) also labeled for the cholinergic marker ChAT (C). More intense ChAT staining was evident in preganglionic varicosities that surrounded many of these neurons (C, insert). (D–F) Confocal images of another section, doubled labeled for CHT (D) and VAChT (E), showed that these cholinergic markers were colocalized (yellow in the overlay, panel F) in varicosities around ICNs and in many atrial nerve fibers (open arrows). Inserts at lower left show boxed regions at higher magnification. Panels (B) and (C) show single optical sections, and panels (D–F) show maximum projection images compiled from an 8 µm confocal series. a – aorta, ra – right atrium, and rv – right ventricle. Scale bars indicate 500 µm in (A) and 100 µm in (B and C) and (D–F).

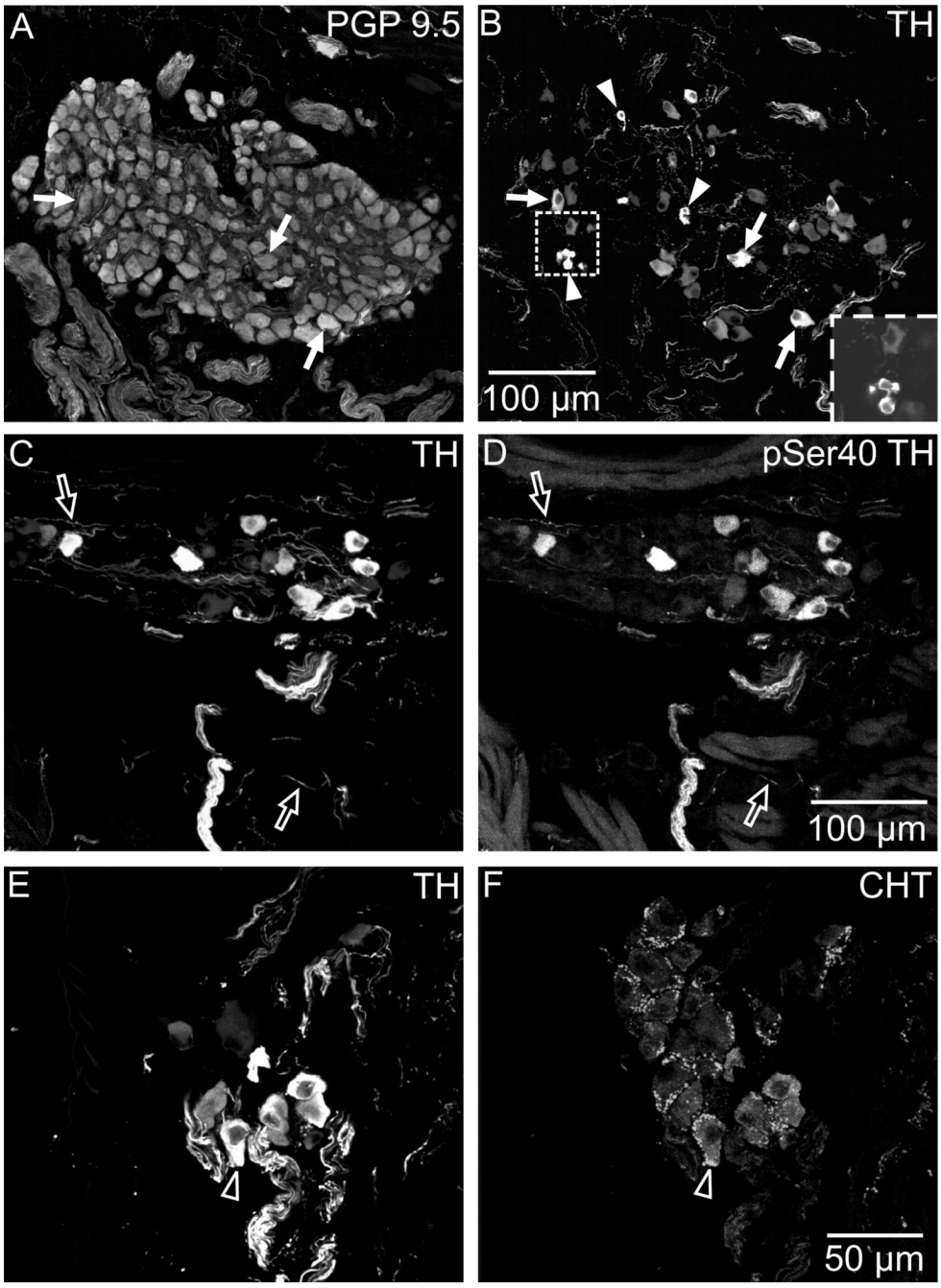

Fig. 2. A subpopulation of mouse ICNs also contained TH and pSer40 TH

Immunohistochemical staining revealed that about 30% of ICNs, identified by PGP 9.5 labeling (A) also exhibited staining for TH (B). Arrows (A and B) indicate examples of neurons that were double-labeled for PGP 9.5 and TH, while arrowheads (B) identify TH-positive SIF cells (single or small clusters) within the ganglion. Insert in (B) shows a single optical section through a cluster of SIF cells. TH and pSer40 TH were colocalized in neurons and in nerve fibers (open arrows in C and D). Double labeling for TH and CHT (E and F) showed that TH-IR neurons (E) were sometimes surrounded by cholinergic varicosities (F). Open arrows indicate the same neuron in E and F. All panels are maximum projection images compiled from

confocal scans, with (A–D) spanning 10 μm each and (E–F) spanning 3.6 μm. Scale bars indicate 100 μm in (A and B) and (C and D) and 50 μm in (E and F).

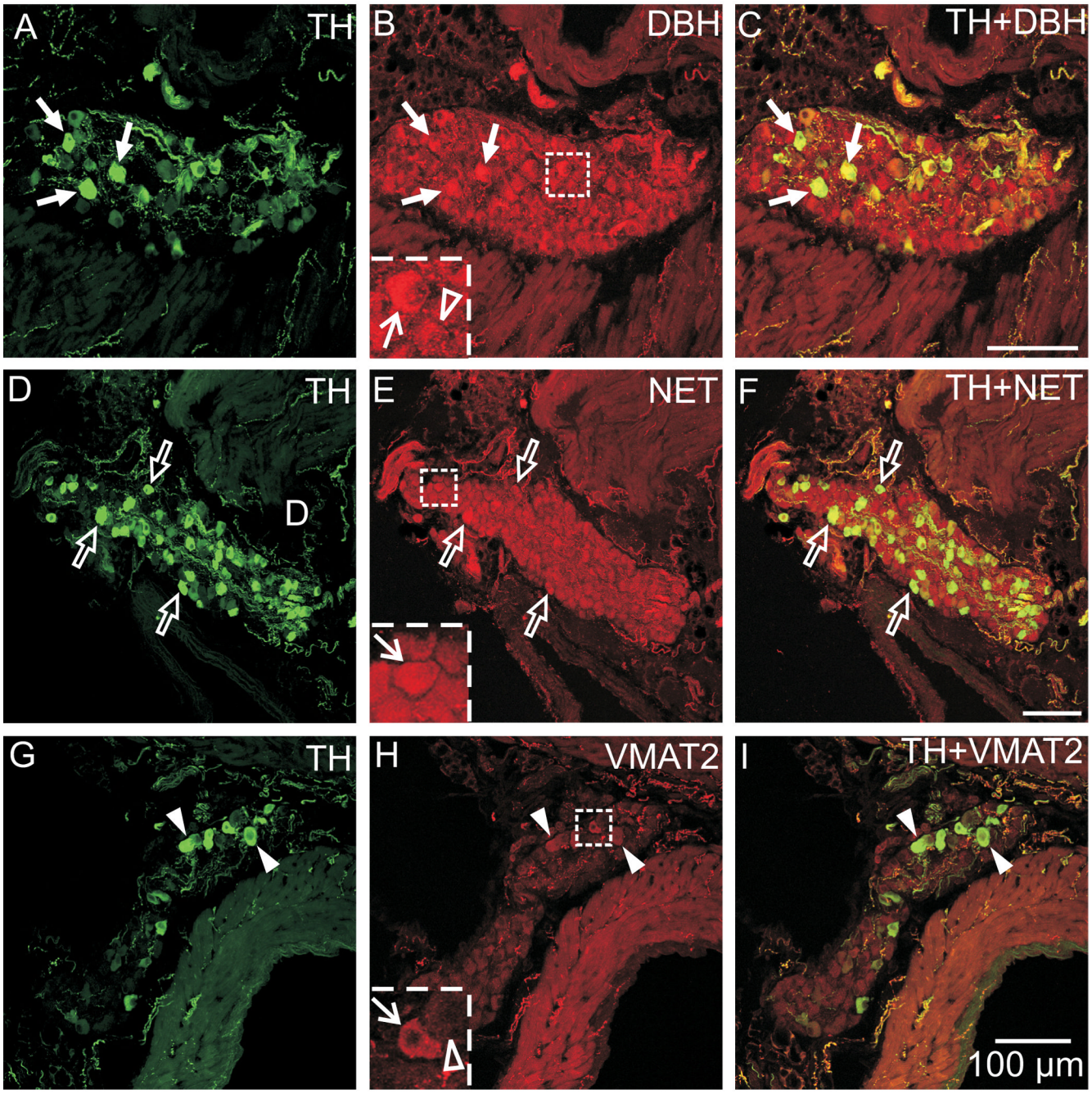

Fig. 3. All ICNs were immunoreactive for DBH and NET but these cells rarely showed VMAT2 immunoreactivity

Double labeling for TH and DBH (A–C) and for TH and NET (D–F) showed that DBH and NET were present in TH-positive and TH-negative ICNs. (A–C) Arrows indicate examples of neurons that contained TH and DBH. The intensity of DBH staining was slightly higher in some TH-positive neurons compared to TH-negative neurons (B insert: line arrow indicates DBH in TH-positive neuron and open arrowhead indicates an adjacent TH-negative neuron with less intense DBH labeling). (D–F) Likewise, NET staining was evident in all neurons, including those that contained TH (open arrows), and was sometimes more intense when colocalized with TH (D insert, line arrow). (G–I) Double labeling for TH and VMAT2 showed

that almost all ICNs lacked VMAT2, although weak VMAT2 staining was rarely observed in THIR neurons (arrowheads). This observation is demonstrated in (H insert), where the line arrow indicates an example of a TH-positive neuron with weak VMAT2 staining and the open arrowhead shows an adjacent cell not containing VMAT2. All panels contain maximum projection images compiled from confocal scans, with (A–C) spanning 5 μm, (D–F) spanning 10 μm, and (G–I) spanning 8 μm. Scale bars indicate 100 μm in (A–C), (D–F), and (G–I).

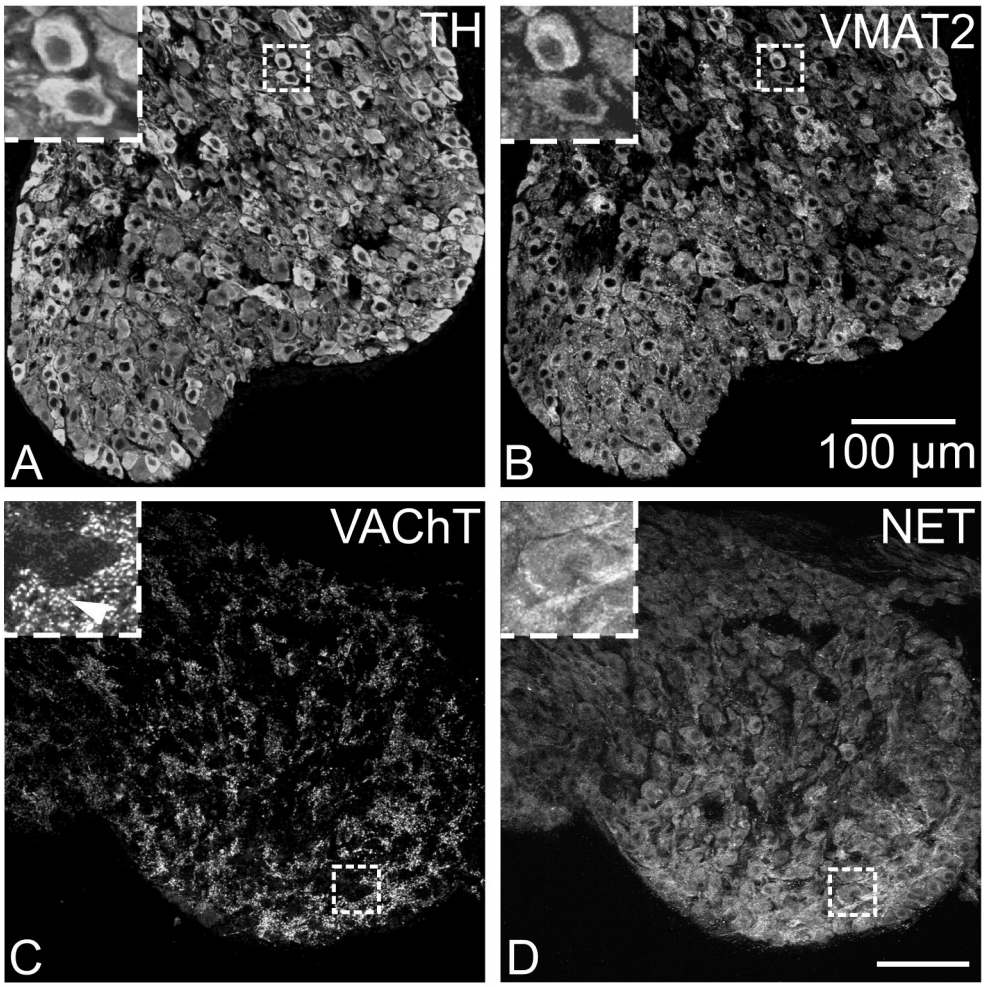

Fig. 4. Immunostaining for noradrenergic markers and VAChT in the stellate ganglion

(A and B) Most neurons in the stellate ganglion stained for TH (A), and unlike ICNs, all of the TH-labeled stellate neurons also stained for VMAT2 (B). (C and D) Stellate neurons also labeled for NET (D) and were surrounded by cholinergic varicosities that contained VAChT (C). Inserts at upper left show boxed regions at higher magnification. Arrowhead indicates VAChT varicosities. All panels show maximum projection images compiled from confocal scans, with (A and B) spanning 3.2 μm and (C and D) spanning 8 μm. Scale bars indicate 100 μm in (A and B) and (C and D).

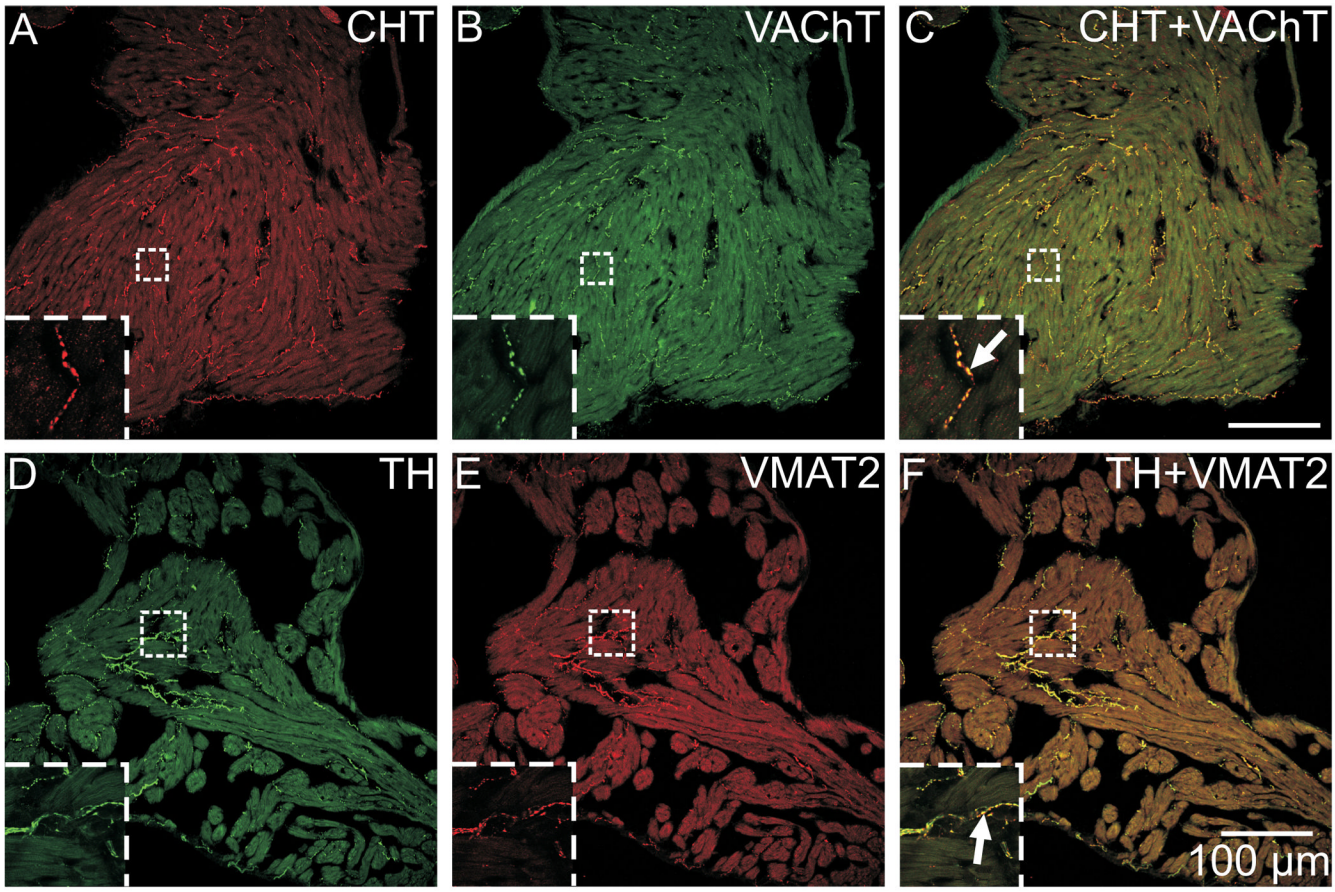

Fig. 5. Colocalization of CHT with VAChT and of TH with VMAT2 in atrial nerve fibers

(A–C) The cholinergic markers CHT (A) and VAChT (B) were localized to identical sites in nerve fibers, resulting in a yellow color at the points of colocalization in the overlay image (C). (D–F) Similarly, the noradrenergic markers TH (D) and VMAT2 (E) were also colocalized in nerve fibers (F). Panels (A–F) show maximum projection images compiled from confocal scans that spanned 8 μm, and inserts show single optical sections from the boxed regions at higher magnification. Scale bars indicate 100 μm in (A–C) and (D–F).

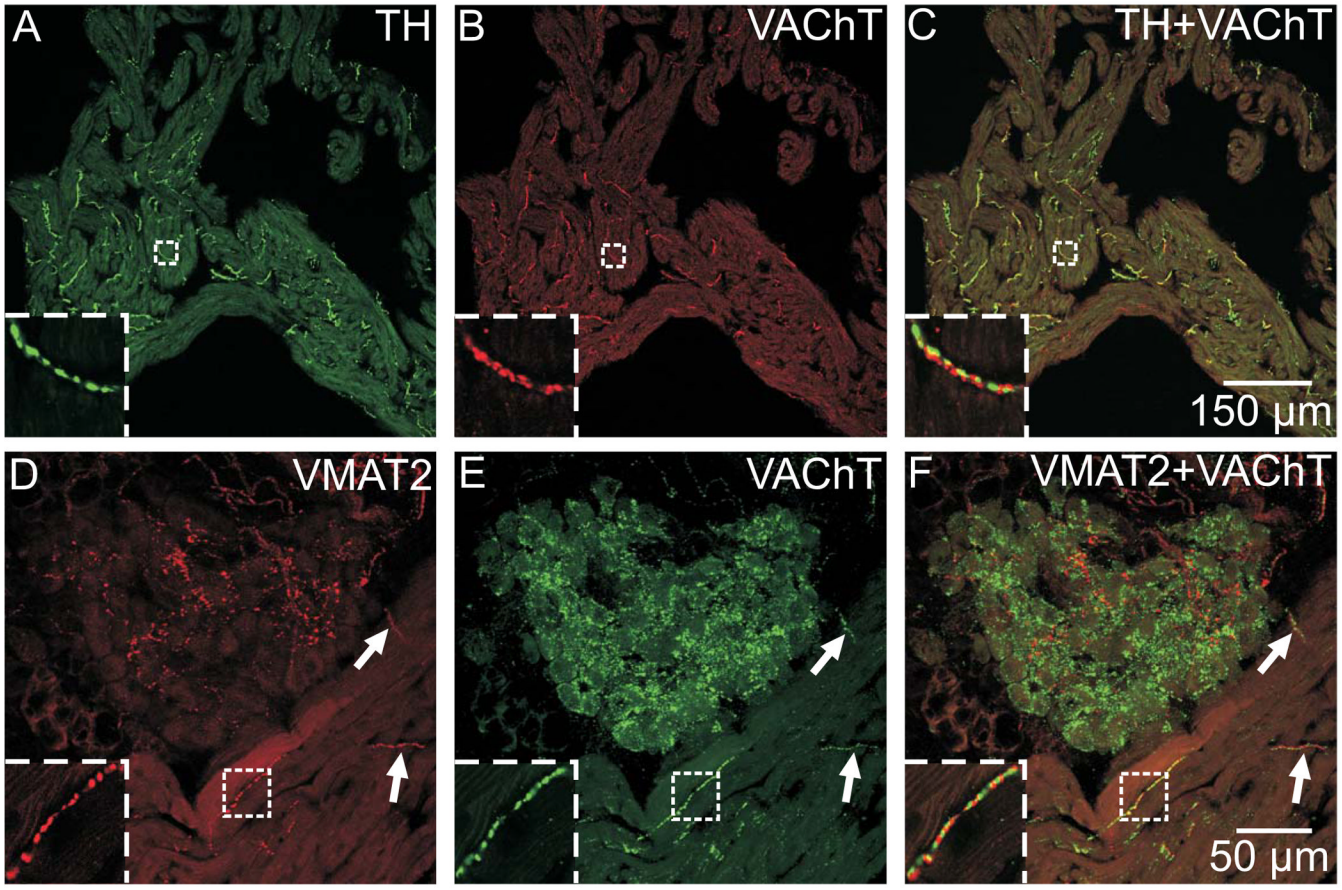

Fig. 6. Cholinergic markers are not colocalized with noradrenergic markers in cardiac nerve fibers

(A–C) Immunostaining for TH (A) and VAChT (B), while located in very close proximity, were not in the same physical space, as evident by the lack of yellow in the overlay image (C). (D–F) Likewise, immunostaining for VMAT2 (D) and VAChT (E) were not colocalized in atrial nerve fibers or nerve fibers within ICG (F). Arrows indicate two examples of nerve fibers in which the labels were obviously not colocalized (F), even at a low magnification. Inserts at lower left show boxed regions at higher magnification. Panels (D–F) show maximum projection images complied from confocal scans spanning 8 μm, while panels (A–C) and all inserts show single optical sections. Scale bars indicate 150 μm in (A–C) and 50 μm in (D–F).

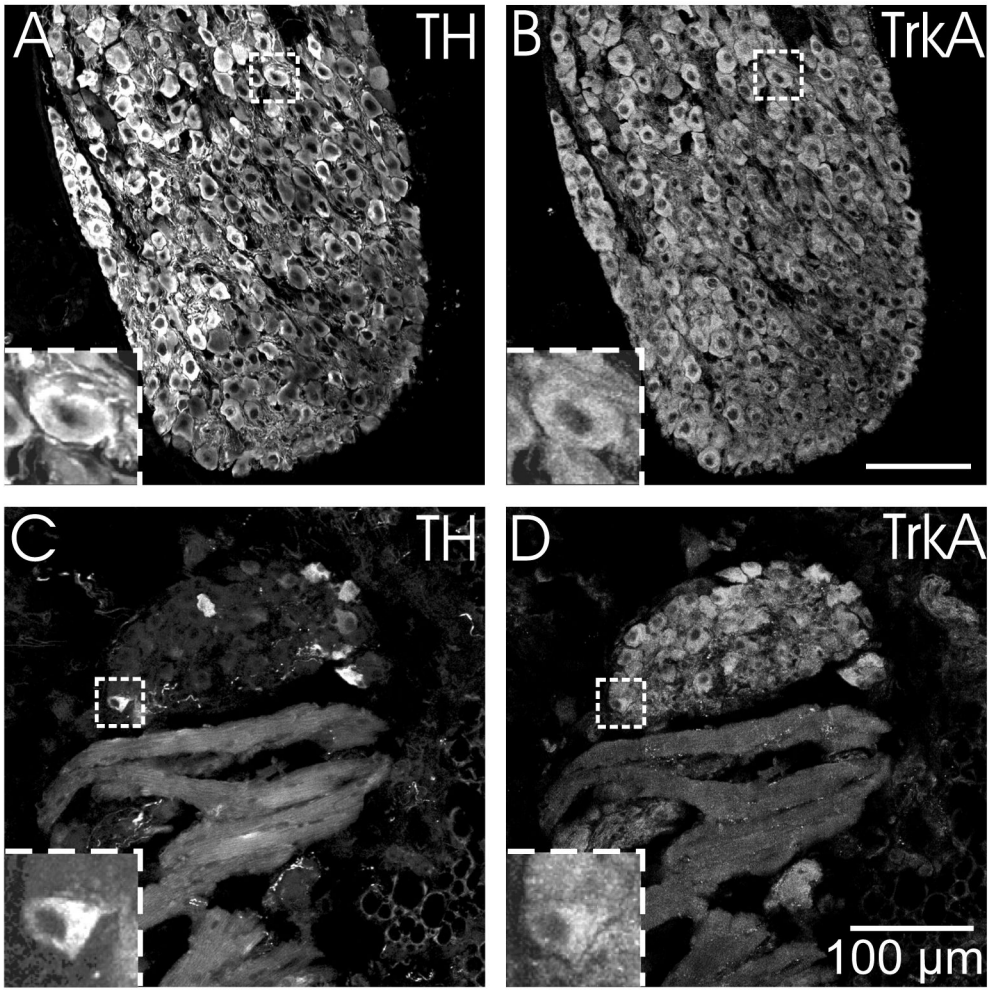

Fig. 7. ICNs and sympathetic neurons of the stellate ganglion show TrkA immunoreactivity

(A–B) All TH-IR neurons in the stellate ganglia (A) were also TrkA-IR (B). (C–D) While only a subpopulation of intrinsic cardiac neurons was TH-IR (C), the entire population of neurons was TrkA-IR (D). TrkA-immunoreactivity was not evident in nerve fibers within the myocardium (D). Inserts at lower left show boxed regions at higher magnification. All panels show maximum projection images compiled from confocal scans spanning 3.2 μm. Scale bars indicate 100 μm in (A and B) and (C and D).

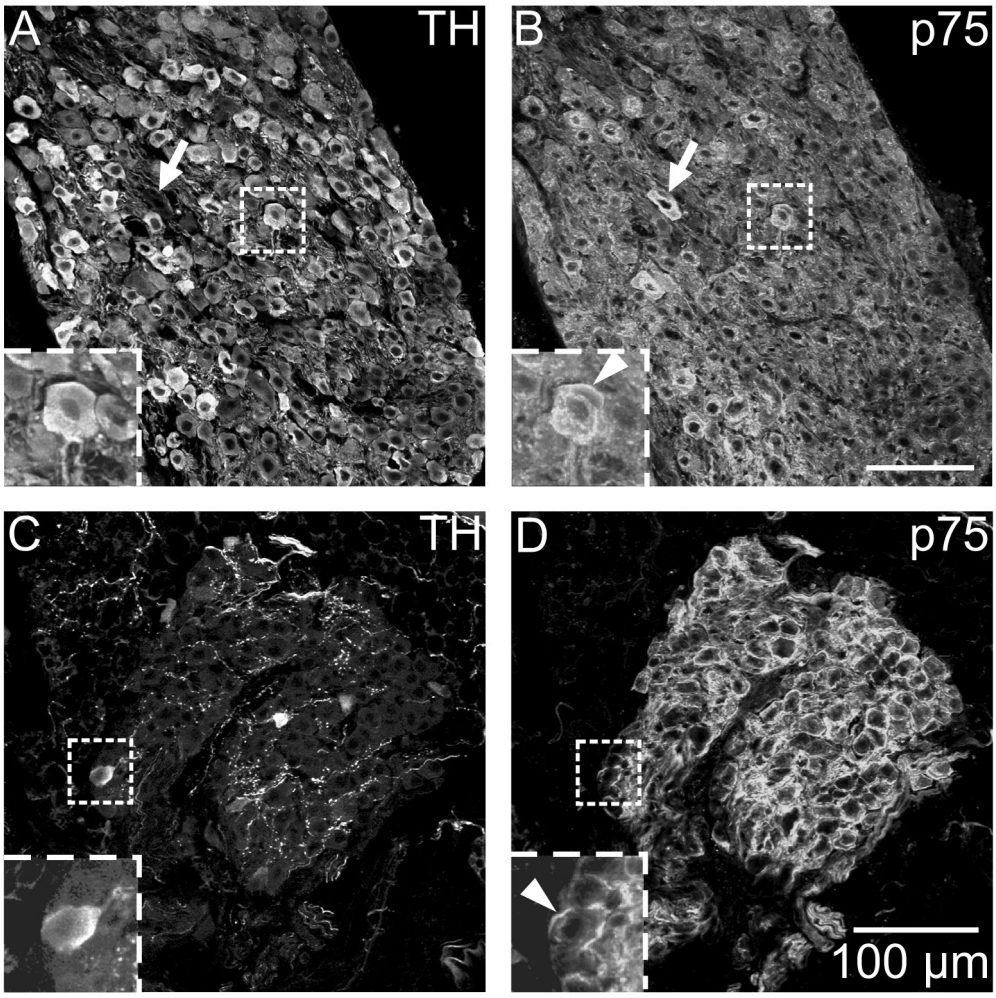

Fig. 8. ICNs and sympathetic neurons of the stellate ganglion show p75 receptor immunoreactivity

(A and B) All TH-IR neurons in the stellate ganglion (A) were also p75 receptor-IR (B). (C–D) While only a subpopulation of ICNs was TH-IR (C), the entire population of neurons was p75 receptor-IR (D). Inserts at lower left show boxed regions at higher magnification. (B and D) Arrowheads indicate prominent p75 staining at the perimeter of neurons. Arrows in A and B indicate a stellate ganglion neurons that was not TH-IR. All panels show maximum projection images compiled from confocal scans spanning 3.2 μm. Scale bars indicate 100 μm in (A and B) and (C and D).

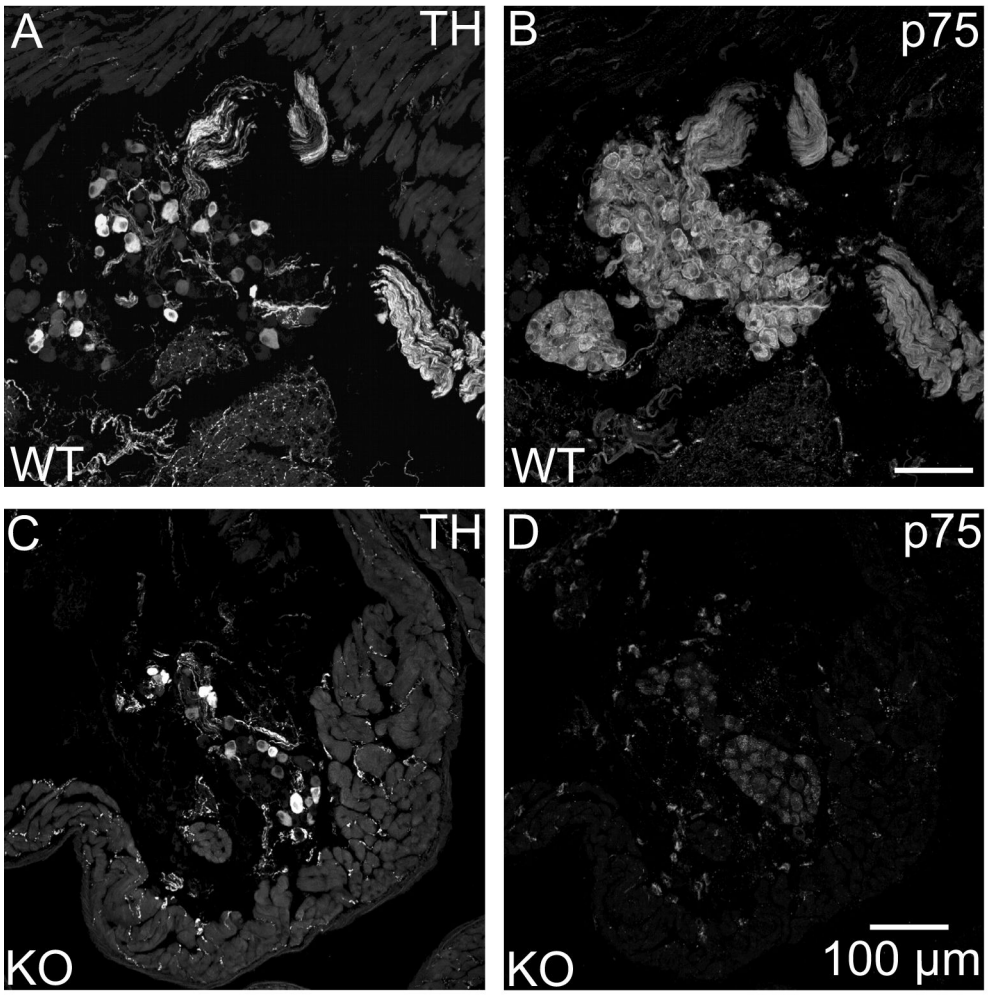

Fig. 9. p75 immunostaining was confirmed as specific through the use of a *p75 receptor* (−/−) mouse

p75 labeling of ICNs and cardiac nerve fibers was present in a wild-type (WT) mouse (B) and absent in a knockout (KO) mouse (D). TH staining of the same sections showed no differences between the WT mouse (A) and the p75 KO (C). All panels show maximum projection images compiled from confocal scans spanning 8 µm. Scale bars indicate 100 µm in (A and B) and (C and D).

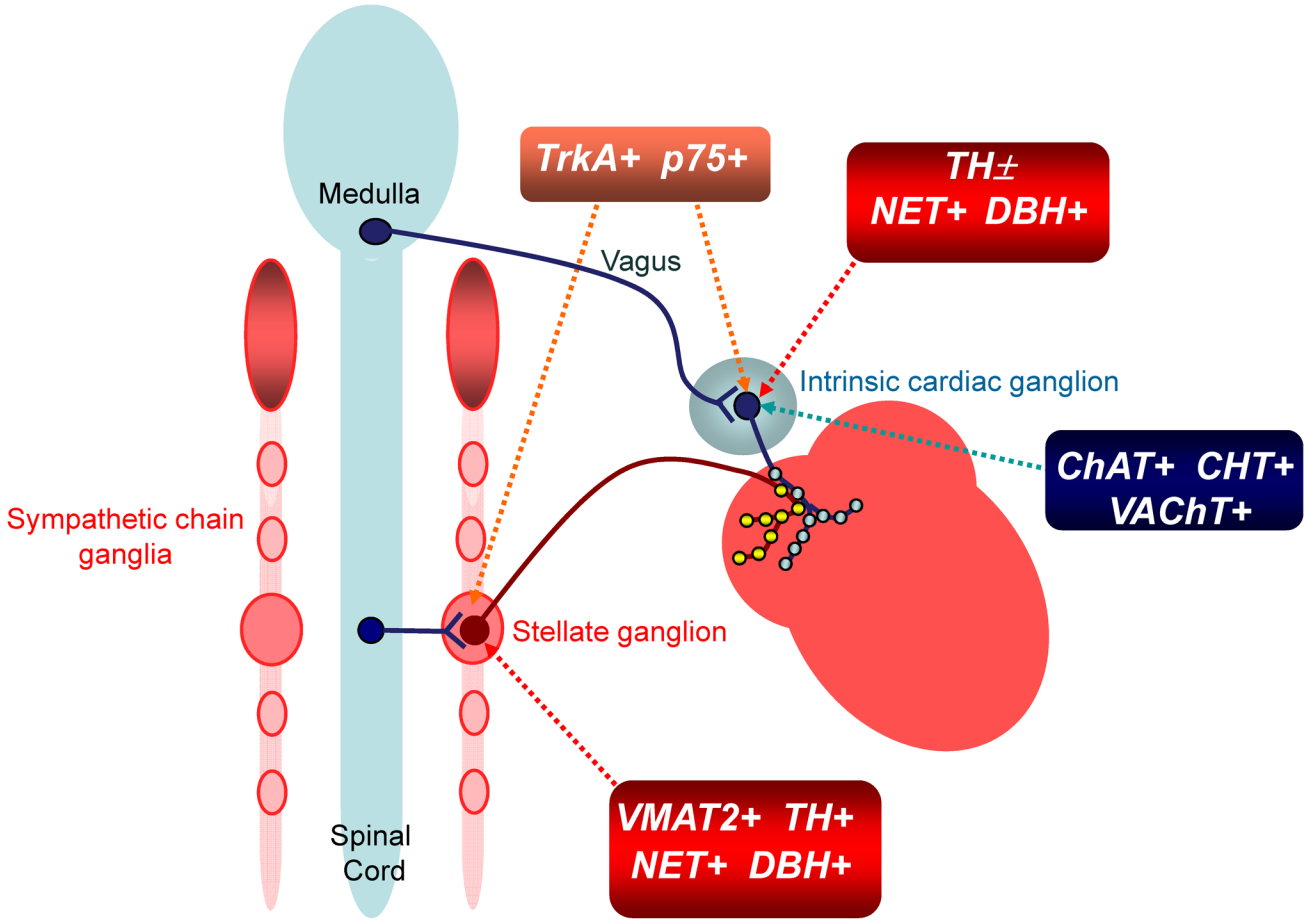

Fig. 10. Diagram showing the neurochemical phenotypes and preganglionic innervation of ICNs and stellate ganglion neurons

ICNs exhibit the cholinergic phenotype (i.e., contain ChAT, CHT and VAChT) and provide cholinergic innervation to cardiac myocytes. They receive cholinergic input from preganglionic vagal efferent neurons located in the medulla. Noradrenergic innervation has its origin in the stellate ganglia and other sympathetic chain ganglia. Most of these neurons exhibit the noradrenergic phenotype (i.e., contain TH, DBH, NET and VMAT2) but only a portion of them innervate the heart. Stellate ganglion neurons receive preganglionic input from cholinergic efferent neurons located in the spinal cord. Noradrenergic neurons also contain TrkA and p75 neurotrophin receptors, which mediate trophic support provided by NGF. ICNs also contain some elements of the noradrenergic phenotype. All “cholinergic neurons” of the ICG contain NET and DBH, and a sizable subpopulation contains TH as well (TH±), but they lack VMAT2. Noradrenergic markers present in ICNs are limited to the soma and may confer the capability for uptake and degradation of catecholamines. ICNs that contain TH might also have the ability to synthesize NE but could not store catecholamines since they lack VMAT2. Release of NE might occur via NET under pathophysiological conditions. Cholinergic nerve fibers are often closely apposed to noradrenergic nerve fibers in the atria, providing the opportunity for crosstalk. Some ICNs also receive input from noradrenergic nerves (not shown), which probably have their origin in sympathetic chain ganglia. All ICNs contain TrkA and p75 receptors, suggesting that they may respond to NGF.

Table 1

Primary and Secondary Antibodies for Immunohistochemistry

Antibody (abbreviation)	Host	Dilution	Supplier	Catalog Number
Choline Acetyltansferase (ChAT)	Goat	1:50	Chemicon (Temecula, CA)	AB144P
High Affinity Choline Transporter (CHT)	Rabbit	1:250	Chemicon	AB5966
Dopamine Beta-Hydroxylase (DBH)	Rabbit	1:1000	Immunostar (Hudson, WI)	22806
Norepinephrine Transporter (NET)	Rabbit	1:500	Randy Blakely	43408
p75	Rabbit	1:300	Advanced Targeting Systems (San Diego, CA)	AB-N01
Protein Gene Product 9.5 (PGP 9.5)	Rabbit	1:1000	Chemicon	AB1761
Tyrosine Hydroxylase (TH)	Sheep	1:1000	Chemicon	AB1542
Tyrosine Hydroxylase (TH)	Rabbit	1:1000	Pel-Freez Biologicals (Rogers, AR)	P40101
Tyrosine Hydroxylase, Ser-40 phosphorylated (pSer40 TH)	Rabbit	1:500	Serotec (Raleigh, NC)	AHP912
TrkA	Rabbit	1:100	Upstate (Lake Placid, NY)	06-574
Vesicular Acetylcholine Transporter (VAChT)	Guinea Pig	1:200	Chemicon	AB1588
Vesicular Acetylcholine Transporter (VAChT)	Goat	1:2000	Chemicon	AB1578
Cy5 AffiniPure Donkey Anti-Guinea Pig IgG	Donkey	1:200	Jackson ImmunoResearch Laboratories, Inc (West Grove, PA)	706-175-148
Alexa Fluor 555 Donkey Anti-Rabbit IgG	Donkey	1:200	Invitrogen (Carlsbad, CA)	A31572
Alexa Fluor 488 Donkey Anti-Goat IgG	Donkey	1:200	Invitrogen	A11055
Alexa Fluor 488 Donkey Anti-Sheep IgG	Donkey	1:200	Invitrogen	A11015